LANGMUIR

Article

pubs.acs.org/Langmuir

Surfactant and Plasticizer Segregation in Thin Poly(vinyl alcohol) Films

Arron Briddick,[†] Peixun Li,[‡] Arwel Hughes,[‡] Florence Courchay,[§] Alberto Martinez,[§] and Richard L. Thompson*[,†]

[†]Department of Chemistry, Durham University, Science Site, Durham DH1 3LE, U.K.

[‡]STFC ISIS Facility, Rutherford Appleton Laboratories, Chilton, Didcot, OX11 0QX, U.K.

[§]Brussels Innovation Center (BIC), Procter & Gamble, Temselaan 100, 1853 Strombeek Bever, Brussels, Belgium

Supporting Information

ABSTRACT: The vertical depth distributions of individual additive components [cetyltrimethylammonium bromide (CTAB), deuterated pentaethylene glycol monododecyl ether (d_{25}-$C_{12}E_5$), and deuterated glycerol (*d*-glycerol)] in PVA films have been isolated and explored by ion beam analysis techniques and neutron reflectometry. The additives display an unexpectedly rich variety of surface and interfacial behaviors in spin-cast films. In separate binary films with PVA, both *d*-glycerol and CTAB were evenly distributed, whereas d_{25}-$C_{12}E_5$ showed clear evidence for surface and interfacial segregation. The behavior of each surfactant in PVA was reversed when the plasticizer (glycerol) was also incorporated into the films. With increasing plasticizer content, the surface activity of d_{25}-$C_{12}E_5$ systematically decreased, but remarkably, when glycerol and CTAB were present in PVA, the surface and interfacial activities of CTAB increased dramatically in the presence of glycerol. Quantification of the surface excess by ion beam analysis revealed that, in many cases, the adsorbed quantity far exceeded what could reasonably be explained by a single layer, thus indicating a wetting transition of the small molecules at the surface or interface of the film. It appears that the surface and interfacial behaviors are partly driven by the relative surface energies of the components, but are also significantly augmented by the incompatibility of the components.

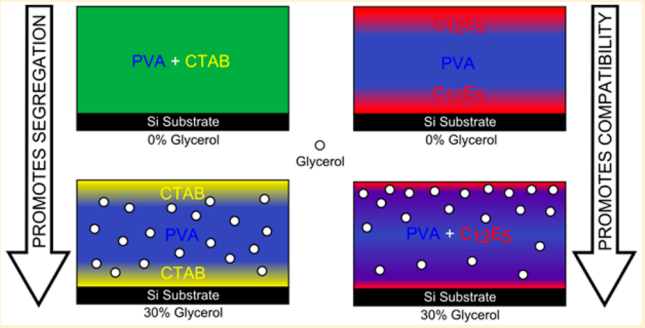

INTRODUCTION

Poly(vinyl alcohol) (PVA) is a semicrystalline synthetic polymer with excellent film-forming ability and optical transparency. PVA is used primarily in food packaging, medical applications, and now increasingly in the laundry industry because of its resistance to organic solvents, aqueous solubility, biodegradability, and low environmental impact. The food-packaging industry has used PVA to prolong the lifetime of stored foods without contamination,[1] and there are many medical applications including both implantable and non-implantable devices.[2−5] PVA's primary use in the laundry industry is the encapsulation of detergent for unit-dose clothes washing. Whereas neat and plasticized PVA materials have been studied extensively, relatively little attention has been devoted to the surface properties of thin PVA films.

PVA cannot be synthesized directly from vinyl alcohol but is instead prepared by the hydrolysis of poly(vinyl acetate) (PVAc), so it is typically a copolymer of PVA with some residual PVAc. The degree of hydrolysis (DH) is a measure of the percentage of —OC(═O)CH_3 acetate groups that have been converted to —OH groups in the final polymer, and the number and positions of residual acetate groups largely determine the properties of the polymer, having the most significant effect on water solubility. Resins with lower DH values (<95%) show a significant increase in solubility because crystallinity is decreased by the presence of more hydrophobic acetate groups, which disrupt the stereoregularity of the polymer chain and do not readily participate in intra-/intermolecular hydrogen bonding.[6] Degree of polymerization has also been shown to be correlated to water solubility, with lower-molecular-weight PVA chains showing greater solubility at ambient temperatures.[7] However, desirable mechanical properties such as tensile strength are also reduced at lower molecular weight,[8] so these characteristics of the resin must be tailored to the application. Although the properties of pure PVA films are extensively customizable through alterations of these parameters, PVA alone is still generally too brittle and inflexible for many uses.

Plasticizers can be introduced to improve film flexibility while maintaining relatively good mechanical properties (tensile, shear strength). In PVA, plasticizers collect in the amorphous regions of the polymer, causing an increase in the free volume

Received: October 14, 2015
Revised: December 23, 2015
Published: December 30, 2015

DOI: 10.1021/acs.langmuir.5b03758
Langmuir 2016, 32, 864−872

and a lowering of the glass transition temperature (T_g). Glycerol is commonly used to plasticize PVA because of its low molecular weight, low volatility, and good compatibility with the host polymer.[9] A truly compatible plasticizer should exhibit a homogeneous distribution throughout the host polymer matrix; hence, mapping of the location of glycerol within PVA can be used to characterize the nature of plasticization. Plasticized films used in industry come into contact with a number of compounds and environments depending on their intended use, and long-term product stability might be compromised by the migration and adsorption of plasticizers into or out of the PVA matrix. Our interest is in determining how small molecules such as surfactants and plasticizers are distributed in simple mixtures with PVA and how this behavior is altered by the complexity of multiple components.

Mixtures of polymers and small molecules are widely applied in plasticized materials for packaging, adhesives, and coatings, and their use in complex formulations is well-characterized, although usually on only an empirical level. There remains a fundamental scientific challenge in predicting the behavior of all but the simplest model systems, as the interplay among different components involves complex interactions among ionic, polar, and nonpolar groups and phenomena arising from these interactions span length scales ranging from atomistic to several microns. The presence of surfaces or interfaces further complicates this situation, although it is at least possible to rationalize the key factors responsible for the preferential segregation of one component over another at an interface. First, the component with the lowest surface energy should be enriched at the surface of a mixture. In the absence of any discernible difference in surface energies, it has been shown that molecular size is significant, with the lower-molecular-weight component being enriched at the surface.[10] The extent of surface segregation is further augmented by reducing the compatibility of the components. In surfactant solutions, it is well-known that increasing the hydrocarbon-chain length of a surfactant in an aqueous solution reduces the equilibrium surface tension by promoting adsorption at lower concentrations.[11] In polymer blends, increasing incompatibility (increasing Flory–Huggins interaction parameter) enhances surface segregation and ultimately leads to the formation of a wetting layer.[12]

Although the surface adsorption of surfactants and polymers in solutions is a mature area of research, the reverse case in which the solvent is replaced by a high-molecular-weight polymer has received less attention. Of particular relevance to our present work is that of Edler and co-workers concerning film-forming polymers and surfactants. In their work, it was noted that significant interactions between ionic groups of cationic surfactants and lone pairs of water-soluble polymer, notably poly(ethylenimine) (PEI) can lead to the formation of complexed films.[13,14] The fact that film formation is spontaneous indicates that surfactant–polymer interactions can have quite dramatic effects on the properties of polymer films, which is the focus of our work. Here, we explore for the first time the surface and interfacial segregation of two model surfactants and a plasticizer in PVA films. For this initial study, we chose model nonionic and cationic surfactants, both of which have been well-characterized as surfactants in aqueous systems. The ion beam analysis and neutron reflection techniques that we have used enable the depth distribution of a single component within a complex mixed film to be isolated. In addition to simple binary polymer + surfactant or polymer + plasticizer mixtures, we also consider the more complex (and industrially relevant) situation of surfactant and plasticizer in a PVA film. Commercial formulations of PVA films interact with plasticizers and surfactants when used in several products; therefore, the distribution of these components is highly relevant to the bulk and surface properties of these materials. Our results show that, even with simple models for complex industrial formulations, a surprisingly rich variety of behaviors can result from their interactions.

EXPERIMENTAL SECTION

Materials and Sample Preparation. PVA resin (Sigma-Aldrich P8136, M_w = 30–70 kg/mol, DH = 87–90%), glycerol (Aldrich), d_5-glycerol (CK Isotopes), and cetyltrimethylammonium bromide (CTAB; Acros Organics, >99%) were purchased and used as received. Pentaethylene glycol deuterated monododecyl ether (d_{25}-$C_{12}E_5$) was prepared at Rutherford Appleton Laboratories according to the method described elsewhere.[15,16]

Aqueous 4% (w/v) PVA solutions were prepared in deionized water by heating to 75 °C and stirring until the resin had completely dissolved. Aqueous solutions of the small molecules glycerol, d_5-glycerol, CTAB, and d_{25}-$C_{12}E_5$ were also made at 4% (w/v). Polymer + surfactant and/or glycerol solutions were then prepared from these stock solutions in defined mass ratios and thoroughly mixed to yield 4% (w/v) solutions from which films could be cast. Films with thicknesses between 150 and 300 nm were prepared by spin-coating the mixed solutions onto fresh silicon wafers. Although the critical micelle concentrations and aggregation behaviors of these surfactants in PVA are not yet known, it is likely that the surfactants might exhibit some aggregation at the concentrations chosen. The concentration range was chosen such that there would be sufficient surfactant present within the films to be detectable. Prior to coating, the silicon wafers were cleaned with acetone to remove any traces of hydrophobic impurities and ensure consistent film production.

Ion Beam Analysis. Vertical concentration profiles of components within the spin-cast films were determined by the ion beam analysis techniques of Rutherford backscattering spectroscopy (RBS) and nuclear reaction analysis (NRA), using a National Electrostatics Corporation 5SDH Pelletron Accelerator with RC43 endstation. The application of ion beam analysis techniques to soft matter is described in greater detail elsewhere.[17,18] During these experiments, sample integrity was maintained by cooling to below −50 °C using a liquid-nitrogen-cooled sample holder. In addition to minimizing sample degradation due to beam damage, this step was essential to retain the low-molecular-weight components in the films under a vacuum ($<4 \times 10^{-6}$ Torr). Because of the low film thickness and macroscopic surface area, evaporation of glycerol and nonionic surfactant under ambient conditions was detectable over a period of hours, so films for ion beam analysis were vitrified by being submerged in liquid nitrogen immediately prior to ion beam analysis experiments.

RBS experiments were carried out using a 1.5 MeV $^4He^+$ ion beam incident on the sample surface at 80° to the sample normal. The energy of backscattered $^4He^+$ ions was determined using a Canberra passivated implanted planar silicon (PIPS) detector with a nominal energy resolution of 17 keV at 170° to the incident beam in a Cornell geometry. The same detector setup was used for NRA experiments, except in this case, a 700 keV $^3He^+$ ion beam was incident on the samples.

RBS is particularly well suited to quantifying the vertical concentration profile of heavy elements in a matrix of lighter elements. In these experiments, the cationic surfactant cetyltrimethylammonium bromide (CTAB) was chosen as a model ionic surfactant. The bromide ion of each CTAB molecule is, by far, the heaviest element present in the samples; therefore, it can be sensitively resolved by RBS. The absence of any other ionic species within the CTAB/PVA films coupled with the requirement of charge neutrality ensured that the Br^- ion depth distribution is representative of the CTAB distribution as a

DOI: 10.1021/acs.langmuir.5b03758
Langmuir 2016, 32, 864–872

whole. Under these experimental conditions, RBS provides a depth resolution of ~15 nm.

The other two species of interest, glycerol and a nonionic surfactant, contain no elements that distinguish them from the PVA matrix, so their deuterium-labeled analogues were used as model materials. Deuterium labeling enabled the depth distributions of these molecules in PVA to be quantified by nuclear reaction analysis (NRA) or neutron reflectometry (NR), while having a minimal impact on their physicochemical properties. NRA experiments were carried out on samples containing deuterium-labeled glycerol and deuterium-labeled nonionic surfactant (d_{25}-$C_{12}E_5$). The glycerol was 1,1,2,3,3-d_5 glycerol, chosen so that only nonlabile C−D hydrogens of the molecule were deuterated but the hydroxyl groups were not. (Isotope exchange between labile OH and OD bonds must be avoided to maintain the ability to resolve the small molecules from the polymers.) For these experiments, samples were irradiated with a beam of 0.7 MeV $^3He^+$ ions at 80° to the sample normal. The energy of the backscattered protons resulting from the reaction between ^3He and ^2H within the polymer was analyzed to determine the composition versus depth profile of the deuterated component. Under these experimental conditions, NRA provides a depth resolution of ~8 nm, which, similarly to RBS, is large compared to the molecular dimensions but sufficient to quantify adsorption of these components at exposed surfaces or buried interfaces. All ion beam analysis data were analyzed with the Surrey University DataFurnace[19] software (WiNDF v9.3.68 running NDF v9.6a) to determine the concentration versus depth profiles, where the densities of PVA and glycerol were assumed to be 1.19 and 1.26 g/cm^3, respectively. Rutherford scattering cross sections were assumed for the RBS analysis, and NRA data were analyzed using the scattering cross sections of Möller and Besenbacher.[20] To avoid overparameterization, model composition profiles were restricted to either two or three layers, for which the composition and thickness were allowed to vary to obtain the best possible fit to the experimental data. Further particulars of data analysis with DataFurnace are discussed elsewhere.[21−23]

Neutron Reflectometry. Vertical concentration profiles of components within the spin-cast films were also determined by the neutron reflectometry (NR) analysis techniques using SURF at the Science and Technology Facilities Council (STFC) facility ISIS. Sample preparation was similar to that for the NRA experiments, except that the films were somewhat thinner (70 nm) to maximize the sensitivity of the measurement to changes in film thickness from the Kiessig fringes in the reflectivity profiles. NR offers significantly better depth resolution (0.5 nm) than is achievable with ion beam analysis, provides a direct measure of film surface roughness, and can be performed under atmospheric conditions. The specular reflectivity, $R(Q)$, was measured from before the critical edge ($Q \approx 0.01$ Å^{-1}) to the point at which the signal is indistinguishable from the background ($Q \approx 0.25$ Å^{-1}). This measurement required three angles of incidence and approximately 2 h of acquisition time per sample to obtain data of sufficient statistical quality over the entire Q range. The latter factor imposes a requirement that films must be stable for at least several hours, as any alteration in film thickness during measurements would make accurate interpretation of the data impossible.

The scattering length densities of the silicon substrate and the organic components in the film are listed in Table 1, along with the approximate value for the native oxide layer, which is consistent with results that have been inferred from previous experiments on silicon substrates.[24−26]

RESULTS

Segregation of Individual Components in PVA Films. The results are generally presented as composition versus depth profiles for individual components within PVA films that were derived from ion beam analysis and neutron reflectometry experiments. For each composition profile presented, the numerical values for the layer composition and thickness are tabulated and have been provided in the Supporting Information.

Table 1. List of Scattering Length Densities (SLDs) for Hydrogenous and Deuterated Materials

component	SLD ($\times 10^{-6}$ Å^{-2})
PVA	0.67
Si	2.07
SiO_x	3.0−3.5
glycerol	0.61
d_5-glycerol	4.65
$C_{12}E_5$	0.13
d_{25}-$C_{12}E_5$	4.47

Nuclear reaction analysis data and fits for d-glycerol in PVA films are shown along with the derived concentration profiles for these mixtures in Figure 1a. This technique allows the depth

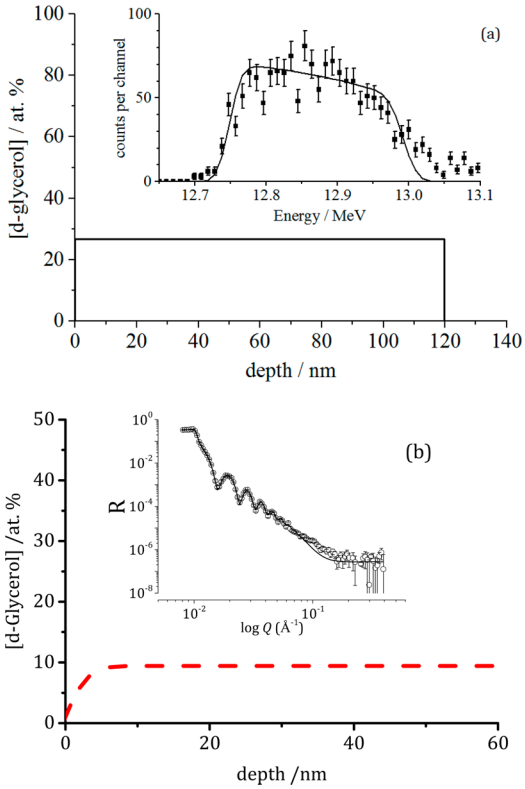

Figure 1. (a) Nuclear reaction analysis data (proton spectrum) for 30% d-glycerol in thin PVA films. The curve fitted to the data (inset) corresponds to the composition versus depth profile of d-glycerol. (b) Neutron reflectometry data and fit (inset) and corresponding composition profile for 10% d-glycerol in thin PVA films.

distribution of a single deuterium-labeled species to be isolated from an arbitrary matrix of other components over a range that can be chosen to be between approximately 100 nm and 10 μm and with a depth resolution of about 5−10% of the range. The sharp onset in the spectrum at 12.77 MeV corresponds to deuterated species present at the film surface, and the gradual decline in proton yield (counts per channel) in this case is due to the decrease in nuclear reaction scattering cross section as the beam penetrates the sample and loses energy. Because of the inverse kinematics of the nuclear reaction in backscattering geometry, protons generated at the surface of the sample are detected at the lowest energy, and protons from greater depths are detected at higher energies.[27] The curve fitted to the experimental data shown in the inset of Figure 1a is the

DOI: 10.1021/acs.langmuir.5b03758
Langmuir 2016, 32, 864−872

calculated proton yield for a homogeneous distribution of d_5-glycerol, as indicated by the flat composition versus depth profile. Note that ion beam analysis is sensitive to composition in terms of "atom" fraction, where molecules are represented by atoms of their average elemental composition. (The mass fractions of the components would be scaled by their relative densities.) The small discrepancy between the model fit and the experimental data at approximately 13.1 MeV indicates some roughness or variation in effective film thickness, which is not taken into account in the model composition profile. Nevertheless, the data are consistent with the d_5-glycerol being evenly vertically distributed within the film. Figure 1b shows complementary NR data for the even distribution of plasticizer throughout the matrix. Although the film studied in this experiment was somewhat thinner and contained a lower loading of d_5-glycerol than the sample examined by NRA, the results are qualitatively similar: The d_5-glycerol is evenly distributed throughout the depth of the film.

In complete contrast to the behavior observed for d_5-glycerol, Figure 2a shows that the nonionic surfactant d_{25}-$C_{12}E_5$ was

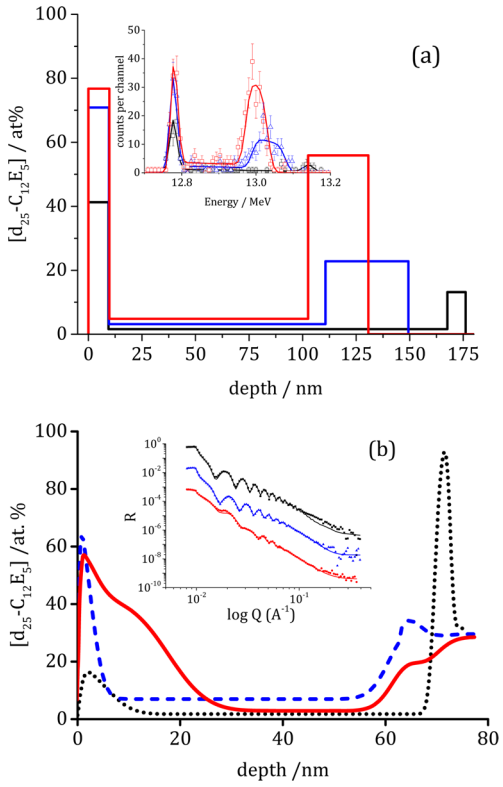

Figure 2. (a) Nuclear reaction analysis data and fits (inset) for 5% (black, squares), 15% (blue, triangles), and 25% (red, circles) d_{25}-$C_{12}E_5$ in thin PVA films. (b) Neutron reflectometry data (offset) and fits for 10% (black, solid squares), 20% (blue, solid triangles), and 30% (red, solid circles) d_{25}-$C_{12}E_5$ in thin PVA films. The derived concentration profiles of d_{25}-$C_{12}E_5$ correspond to the fitted curves.

found to be very unevenly distributed within the PVA film. The large peak in counts per channel near 12.77 MeV corresponds to a significant surface excess of the surfactant, where surface excess is defined as

$$z^* = \int_0^\infty \varphi(z) - \varphi_b \, dz \quad (1)$$

Here, φ_b is the bulk concentration adjacent to the surface excess region, and $\varphi(z)$ is the depth- (z-) dependent volume fraction profile of the near-surface region. The fit to the experimental data yields the composition profile shown in the inset, from which z^* can be calculated. The NR data presented in Figure 2b confirm the presence of surface and interfacial excesses of d_{25}-$C_{12}E_5$ in PVA that formed spontaneously during spin-casting and were stable for at least the duration of the measurements. Furthermore, NR is able to resolve the precise composition profile of the surface and interfacial regions and indicates that the surface and interfacial excess layers are typically not pure surfactant but contain a significant amount of PVA as well. Although the possibility of lateral phase separation cannot be excluded completely, the fact that the NR data can be fitted with a simple wetting-layer model that is consistent with the expected overall composition makes such a possibility seem very unlikely.

The depth distribution of a cationic surfactant, CTAB, in PVA film is revealed by the RBS results shown in Figure 3. The

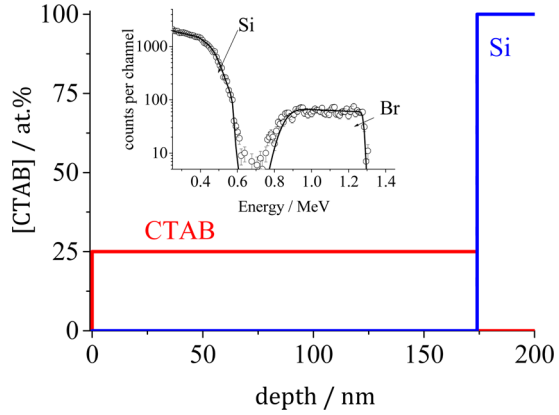

Figure 3. Depth distribution of CTAB in thin, spin-cast PVA films. The inset shows the RBS data and fits for thin films from which the profile was determined.

solid curve fitted to the data in the inset corresponds to the concentration profile of the main figure. In this case, the scattering observed in the region of channels below 0.6 MeV is due to the lighter elements in the sample, namely, C, O, and Si, of which Si makes the dominant contribution. Scattering observed from 0.7 to 1.3 MeV arises from the Br^- ions in the CTAB surfactant.

The low-energy edge of the RBS spectrum corresponding to Br^- at about channel 100 is noticeably more diffuse than the high-energy edge for surface Br^-. Some evidence of film roughness is apparent from the relatively diffuse tail in the RBS spectrum at about 0.8 and 0.55 MeV, which correspond to the elemental composition profiles of the deepest Br^- and the Si closest to the film surface, respectively. By fitting a film roughness of 10% of the total film thickness,[28] both of these features can be captured by the DataFurnace fit to the experimental data. Most significantly, the CTAB in PVA is remarkably evenly distributed throughout the 187-nm film. There is no evidence for surface segregation, which would be apparent as a sharp peak at about channel 1.3 MeV. The calculated surfactant concentration obtainable from Figure 3 is 25%, which is in good agreement with the nominal composition of the spin-cast film.

DOI: 10.1021/acs.langmuir.5b03758
Langmuir 2016, 32, 864−872

Influence of Glycerol Plasticizer on d_{25}-$C_{12}E_5$ Nonionic Surfactant. Even though the d_5-glycerol plasticizer shows no inherent surface segregation itself, the presence of glycerol in the PVA film has quite a profound and unexpected impact on the distributions of the surfactants. Figure 4 shows NRA data

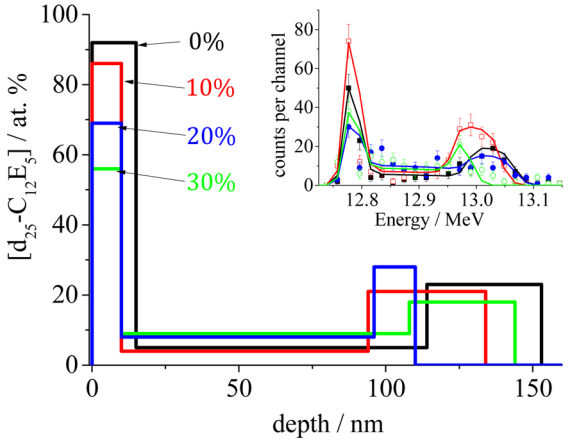

Figure 4. Concentration profiles of 30% d_{25}-$C_{12}E_5$ in mixed PVA/glycerol films as a function of glycerol content. Glycerol concentrations are indicated in the main figure. NRA data and fits are shown in the inset.

and fits for the influence of (hydrogenous) glycerol on the depth distribution of d_{25}-$C_{12}E_5$ in PVA. The mass fraction of surfactant was maintained at 30%, and the mass fraction of glycerol was systematically increased by replacing some of the PVA in the film with glycerol. With increasing glycerol concentration, the surface activity of the nonionic surfactant systematically decreased. This is evident from the reduction in the relative size of the surface excess peak at ~12.77 MeV in the NRA data when compared to the protons detected at higher energies corresponding to d_{25}-$C_{12}E_5$ that is deeper within the PVA film. The model composition profiles determined from fits to the NRA data enable this effect to be quantified. Using neutron reflectometry, the influence of glycerol on the nature of the surface excess profile was investigated. In addition to confirming the result obtained by NRA, the near-surface composition profiles presented in Figure 5 show that the primary influence of glycerol is on the surface concentration, rather than on the spatial extent of the surface enriched layer. Furthermore, the high sensitivity of NR was able to show that, when the isotopic labeling was reversed, the d_5-glycerol was enriched at the surface of $C_{12}E_5$ + PVA films.

Although it is clear that glycerol has the effect of reducing the surface activity of $C_{12}E_5$, it appears that the same plasticizer has the opposite influence on the distribution of CTAB (Figure 6). Here, the addition of glycerol to PVA induces a dramatic change in the RBS spectra, with significant peaks emerging in the parts of the spectra corresponding to surface and interfacial bromide. The roughness was only marginally greater than was observed for the glycerol-free film, with values of 11−16 nm being determined from the RBS analysis. In other words, we found significant levels of both surface and interfacial activity in the CTAB, when glycerol was added to the formulation, even though neither CTAB nor *d*-glycerol showed any discernible segregation when present in isolation in PVA. Thus far, the effect of plasticizer on surfactant was studied; a secondary experiment was carried out with NR to determine the effect of

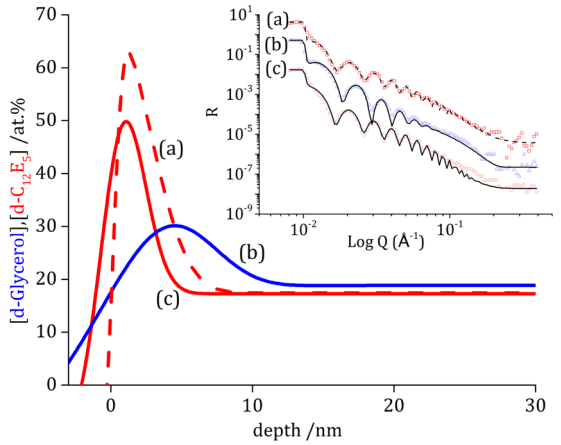

Figure 5. NR data, fits, and composition profiles for (a) 20% d_{25}-$C_{12}E_5$ in PVA, (b) 20% d_5-glycerol and 20% $C_{12}E_5$ in PVA, and (c) 20% d_{25}-$C_{12}E_5$ and 20% glycerol in PVA. The composition profiles are for the singly deuterated component in each case.

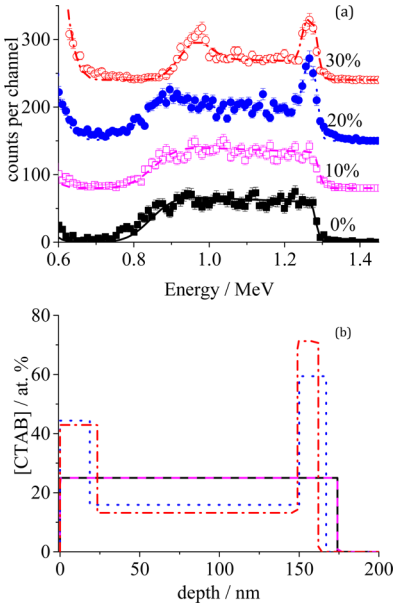

Figure 6. (a) RBS data and fits for the depth distribution of 25% CTAB in mixed PVA/glycerol films as a function of glycerol content. Data are offset for clarity and annotated with glycerol content. (b) Concentration profiles corresponding to the DataFurnace fits: black (0%), mauve (10%), blue (20%), red (30%).

surfactant on the plasticizer distribution. The same results were found in binary films of *d*-glycerol and PVA: In the absence of surfactant, *d*-glycerol showed no surface activity. However, upon introduction of hydrogenous (nondeuterated) $C_{12}E_5$ into the system, which is similar in scattering length density (SLD) to the PVA matrix, leaving *d*-glycerol as the only labeled species, the concentration profile of *d*-glycerol took a form that was remarkably similar to that of the nonionic surfactant (Figure 5b).

DISCUSSION

Surface Enrichment in Two-Component PVA Films. It is well-documented[29,30] that glycerol is sufficiently compatible with PVA to be an effective plasticizer, and our results are also consistent with a single-phase mixture in that the depth

DOI: 10.1021/acs.langmuir.5b03758
Langmuir 2016, 32, 864−872

distribution is at least vertically homogeneous. Surface adsorption, on the other hand, is the defining feature of surfactants; furthermore, blooming of plasticizers to surfaces is also is well-known for many materials. Therefore, some level of surface enrichment of these molecules at the surface of PVA film might still be expected. In the following discussion, we address some of the underlying physical causes of surface segregation to evaluate their contributions to the observed behavior.

In these mixtures of relatively large (PVA) and smaller (glycerol or surfactant) molecules, there is a configurational entropy penalty associated with the deformation of larger molecules at a planar surface; therefore, some surface and interfacial segregation of the smaller molecules might be expected. However, this is a relatively weak effect, and in single-phase mixtures, the levels of surface adsorption are limited to partial coverage[10] and have a correlation length of τ, which is given by

$$\frac{1}{\tau^2} = \frac{\phi_2}{{R_1}^2} + \frac{\phi_1}{{R_2}^2} \tag{2}$$

where ϕ_i is the bulk volume fraction of the ith component and R_i is the characteristic dimension of this component.[31] From the data of Brandrup and Immergut,[32] we obtain the expression for the radius of gyration of PVA as

$$R_g/\mathrm{nm} = 0.0388{M_w}^{1/2} \tag{3}$$

where M_w is the molecular weight in g/mol, yielding a value of approximately 6.7−10.5 nm for the PVA used in this work. Because d-glycerol has an R_g value of approximately 0.5 nm, the correlation length of any adsorbed layer with 30% d-glycerol in PVA would be dominated by this smaller component, and τ would be on the order of 0.6 nm. This value is very small compared to the depth resolution of NRA. Although we cannot exclude the possibility of some enrichment of d-glycerol at PVA surfaces, our NRA results at least confirm that the plasticized film is behaving as a single-phase mixture.

The concentration profiles of CTAB in PVA were qualitatively identical to those of glycerol, which is much more surprising. First, the RBS measurement is more sensitive than NRA because of the strong sensitivity of Rutherford backscattering to heavy elements such as bromine, especially at the surface of a film of light elements. We can predict that even a partial monolayer of CTAB would fall within the detection threshold of the measurement, and this is demonstrated in a quantitative simulation provided in the Supporting Information. Moreover, as a surfactant, CTAB might be expected to display some surface or interfacial activity. Our results appear to suggest that the propensity of small molecules to segregate to the surface is overwhelmed by some more significant factor. We therefore turn our attention to the surface energies of the components present in the films.

The PVA surface energy has been shown to vary with DH and M_w.[33] Two sources quote the surface energy of PVA as 37 mN/m at 20 °C,[34,35] but values of 42−59 mN/m have been given by others.[36−38] The surface energy of PVA decreases with decreasing DH and M_w, and because the PVA used in this study is classified as "partially hydrolyzed" (contains at least 10% PVAc), the surface energy is likely to be at the lower end of the range of values established by other authors. In comparison, glycerol has a surface tension value of 63.4 mN/m at 20 °C,[39] much higher than that of the surface of PVA. In this case, adsorption would not cause any reduction in surface energy, so it is not expected to be spontaneous.

Although there is considerable variation in the energy values for PVA in the literature, all are much lower than the surface tension of water. If CTAB adsorption does not significantly reduce the surface energy of the PVA film in which it is dispersed, then there would be little thermodynamic impetus for this process to occur spontaneously. We are unaware of any measurement of the surface energy of CTAB in the pure state, and the relevance of such a measurement for an ionic solid to the dispersed and dissociated surfactant in PVA is questionable. However, the surface activity of CTAB has been rigorously studied in aqueous solutions, where this surfactant can reduce the surface tension from 72 mN/m to a limiting surface tension [at concentrations above the critical micelle concentration (cmc)] of 32−36 mN/m.[40] The lower values were obtained when KCl was added to the solution, which has the effect of screening the charged groups of the surfactant, enabling closer CTAB packing on the solution surface. In our case, no such additional ions were present, so although we should be cautious in comparing the surface energy of PVA to that of a CTAB solution above the cmc, it is plausible that the lack of adsorption of CTAB at the PVA−air surface is due to their relatively similar surface energies.

In contrast to the results for the plasticizer and cationic surfactant, our NRA and NR experiments showed clear surface segregation of the nonionic surfactant d_{25}-$C_{12}E_5$ to the surface of PVA films. A powerful feature of NRA is that it allows the surface excess of a surfactant to be determined directly, and it appeared that there was a layer of ∼8 nm of almost pure deuterated surfactant at the air surface. The magnitude of the surface excess is highly significant, because it far exceeds the maximum value obtainable for a dense monolayer of the surfactant. The maximum all-trans length of a $C_{12}E_5$ molecule is ∼3.7 nm, and this defines the limiting value of adsorbed layer thickness that could exist if the surfactant molecules were oriented perpendicular to the film surface. Because the measured surface excess is approximately twice this value, it accounts for the equivalent of approximately two end-to-end molecules. Both experimental and computational studies of $C_{12}E_5$ adsorption on water indicate that it forms single layers with the hydrophobic tails outermost and somewhat tilted with respect to the sample normal.[15,41] Although NRA lacks the resolution required to characterize the orientation of the d_{25}-$C_{12}E_5$ chains, it does unambiguously reveal the presence of multilayer adsorption at the surface, which signifies the presence of a wetting layer of surfactant coexisting with the PVA-rich film beneath it.

Surface tension and surface energy arguments can again help to rationalize this phenomenon: $C_{12}E_5$ has a limiting surface tension of 29.9 mN/m at concentrations of ≥0.1 mM in water,[42] which is appreciably lower than the equivalent measure of any other component under consideration. It therefore seems likely that surface adsorption of d_{25}-$C_{12}E_5$ in PVA is favored by the reduction in surface energy associated with this process and is considerably enhanced by the relatively poor compatibility of these materials. Inspection of the composition profiles in Figure 2 suggests that the maximum concentration of d_{25}-$C_{12}E_5$ in PVA in the bulk of the film is approximately 10%, which could be taken as an upper limit to the binodal composition of the mixture.

Influence of Plasticizer on Surface Properties of Three-Component PVA Films. To resolve the origin of the

DOI: 10.1021/acs.langmuir.5b03758
Langmuir 2016, 32, 864−872

large surface excess of d_{25}-$C_{12}E_5$ in PVA films, the impact of replacing some fraction of the PVA with (hydrogenous) glycerol was explored. Both the NRA and NR experiments in Figures 4 and 5, respectively, clearly showed that, when some of the PVA in the film was replaced with glycerol, there was a fairly systematic decrease in the surface excess of d_{25}-$C_{12}E_5$. Schematic representations of the distributions of small molecules (glycerol and surfactant) in PVA for each of the two surfactants studied can be found in Figure 7 (d_{25}-$C_{12}E_5$)

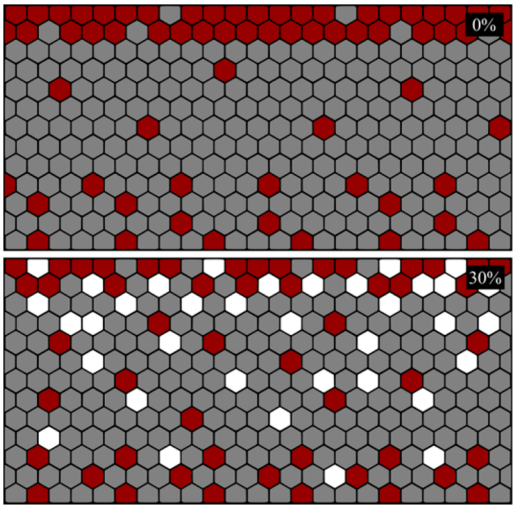

Figure 7. Schematic representation of the effects of glycerol addition (white) on the d-$C_{12}E_5$ (red) distribution in PVA (gray). The plasticizer concentration for each film is given in the upper right corner.

and Figure 8 (CTAB), for which the opposite trend was seen. The surface excess values calculated from the NRA experiments, in which the bulk composition of the film was taken to be the composition of the middle region adjacent to the surface excess, are presented in Figure 9. This decrease cannot be explained if the driving force for d_{25}-$C_{12}E_5$ surface adsorption were purely due to the difference in surface tension. We can

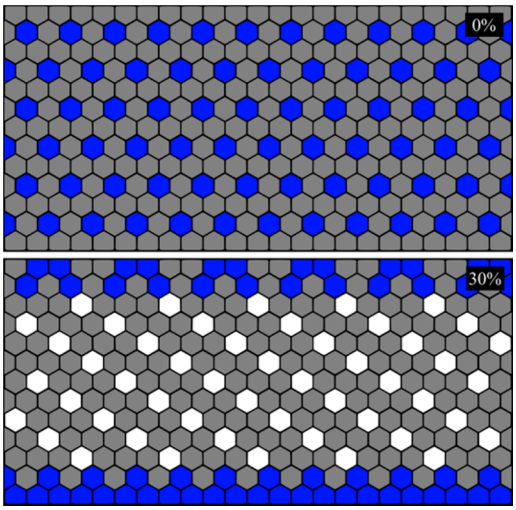

Figure 8. Schematic representation of the effects of glycerol addition (white) on the CTAB (blue) distribution in PVA (gray). The plasticizer concentration for each film is given in the upper right corner.

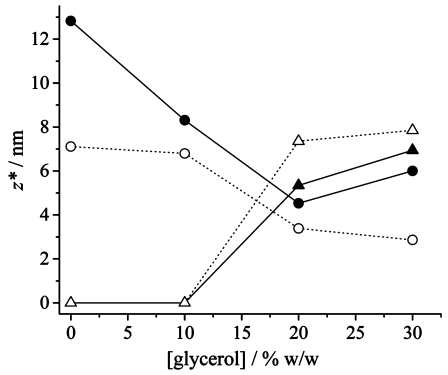

Figure 9. Comparison of the surface excess (solid symbols and solid lines) and interfacial excess (open symbols and dotted lines) of d_{25}-$C_{12}E_5$ (circles) and CTAB (triangles) in PVA films as a function of added glycerol concentration.

draw this conclusion because glycerol has a higher surface tension than any of the reported surface energy values for PVA. On this basis, it is evident that the surface segregation seen for d_{25}-$C_{12}E_5$ in PVA and PVA/glycerol mixtures might be directed by differences in surface energy, but the extent of segregation arises largely from the incompatibility between the surfactant and the other components.

Furthermore, it appears that glycerol leads to an increase in compatibility of d_{25}-$C_{12}E_5$ with the matrix, increasing the solubility of the surfactant and thus decreasing the proportion of surfactant that segregates to the film surface. The relatively high compatibility of d_{25}-$C_{12}E_5$ in glycerol is further supported by the evidence of the NR experiment in which glycerol was the only labeled component (Figure 5). In this case, the contrast in SLD between the PVA and the $C_{12}E_5$ is nearly an order of magnitude smaller than the contrast between the d_5-glycerol and these components; therefore the NR signal is completely dominated by the depth distribution of the plasticizer. In the absence of $C_{12}E_5$, d_5-glycerol was found to have no surface activity in PVA films (Figure 1), but it is clear from Figure 5 that glycerol becomes surface-active when $C_{12}E_5$ is also present. We can therefore conclude that the compatibility between $C_{12}E_5$ and glycerol causes them to become colocated; the $C_{12}E_5$ induces some surface segregation of the glycerol, and the glycerol, being relatively compatible with PVA also, enables more $C_{12}E_5$ to be distributed throughout the bulk of the PVA film.

Given the tendency of glycerol to suppress the surface segregation of d_{25}-$C_{12}E_5$ in PVA, the increase in the surface and interfacial activities of CTAB in PVA with increasing glycerol content, which is apparent from the appearance of the peaks in the RBS data in Figure 6, is quite surprising. The surface and interfacial excess values derived from the composition profiles are shown in Figure 9. The surface activity of CTAB depends on surface tension of the medium in which it is dispersed. In this case, the medium is a mixture of PVA and glycerol, for which the surface tension would be dominated by that of the lower-surface-tension component, PVA. Increasing the amount of glycerol in the PVA should not significantly increase the surface tension of the mixture; therefore it is unlikely to drive the dramatic dependence of surface activity on glycerol content. It is most likely that CTAB is much less compatible with PVA when it is plasticized with glycerol than when it is in its pure state. The reason for this is still not clear, but we speculate that glycerol outcompetes CTAB for its favorable interaction with

DOI: 10.1021/acs.langmuir.5b03758
Langmuir 2016, 32, 864−872

amorphous regions of PVA. Although unresolvable from the presented ion beam analysis results, it seems plausible that CTAB cations bind to the lone pairs of PVA hydroxyl groups in a manner similar to that reported previously for film-forming mixtures of CTAB and imine groups of PEI.[14] It would be interesting to explore whether similar mesostructures such as cylindrical micelles are formed between CTAB and PVA, as these might considerably reduce the mobility of CTAB and, so, inhibit the surface segregation in unplasticized films.

An interesting consequence of the diametrically opposed changes in surfactant solubility in PVA as a function of plasticizer content is that the barrier properties of this film with respect to different surfactants might also follow this pattern; that is, unplasticized PVA might be a relatively good barrier with respect to nonionic surfactants such as $C_{12}E_5$, whereas plasticized PVA might be a better barrier with respect to cationic surfactants.

Interfacial Segregation of Surfactants. Our discussion has so far focused on the segregation of surfactants at the exposed surfaces of PVA films in the presence and absence of plasticizer, but it is noticeable that, in many cases, the surfactant species was also found to be enriched at the buried interface between the film and the silicon oxide surface of the silicon wafer substrate. The magnitude of the excess of surfactant at the silicon oxide interface is comparable to that of the surface excess, although perhaps having a more diffuse distribution. These values are compared in Figure 9. This phenomenon has significance because it further supports the case for surface and interfacial segregation being driven by incompatibility, leading to phase-separated wetting layers on the film surface. The observed concentration profiles are consistent with the profiles seen for surface-directed spinodal decomposition in polymer blends by several authors in the 1990s.[12,43−45] The formation of wetting layers on silica is perhaps also significant in the context of some applications where silica particles can be added to PVA films to prevent cohesion between PVA surfaces. Our results indicate that some combinations of plasticizer and surfactant in PVA could lead to the silica particles becoming engulfed by the surfactant and reduce their effectiveness in this application.

CONCLUSIONS

We have explored the surface and interfacial segregation behaviors of two surfactants and one plasticizer in PVA films by a variety of ion beam analysis techniques and neutron reflectometry, which allow the surface excesses of individual components to be isolated from these mixtures. In binary mixtures with PVA, neither the model plasticizer (*d*-glycerol) nor a cationic surfactant (CTAB) showed any discernible surface segregation within the detection limit of the measurements. However, d_{25}-$C_{12}E_5$ was found to be strongly segregated to the exposed (air) surface of PVA films, and the surface excess was quantified by NRA. It appears that the surface segregation is directed by differences in surface energy but augmented by the incompatibility of the surfactants with the matrix in which they are dispersed. The presence or absence of surface segregation is therefore consistent with the relatively low limiting surface tension of $C_{12}E_5$ solutions, somewhat higher limiting surface tension of CTAB, and significantly higher surface tension of glycerol. The addition of glycerol plasticizer to the PVA + surfactant mixed films has some dramatic and unexpected effects: The surface activity of d_{25}-$C_{12}E_5$ systematically decreases with increasing glycerol content, whereas the opposite effect was observed when glycerol was included in the PVA + CTAB films. We therefore attribute these effects to the different compatibilities of these surfactants with glycerol and the surface segregation being driven significantly by incompatibility. These opposing trends with respect to plasticizer content have significant implications for the barrier properties of plasticized PVA films with respect to surfactant mixtures, as well as the application of inorganic nanoparticles on PVA films to inhibit cohesion.

ASSOCIATED CONTENT

Supporting Information

The Supporting Information is available free of charge on the ACS Publications website at DOI: 10.1021/acs.langmuir.5b03758.

Tables of fitted values for ion beam and NR experiments and figure illustrating the sensitivity of RBS measurements (PDF)

AUTHOR INFORMATION

Corresponding Author

*E-mail: r.l.thompson@durham.ac.uk.

Notes

The authors declare no competing financial interest.

ACKNOWLEDGMENTS

We are grateful to EPSRC/Procter and Gamble (U.K.) for supporting this project through an industrial CASE award (EP/L505419/1). We are also grateful to STFC for the provision of the neutron reflection facilities.

REFERENCES

(1) Tripathi, S.; Mehrotra, G. K.; Dutta, P. K. Physicochemical and bioactivity of cross-linked chitosan−PVA film for food packaging applications. *Int. J. Biol. Macromol.* **2009**, *45*, 372−376.

(2) Ma, R.; Xiong, D.; Miao, F.; Zhang, J.; Peng, Y. Novel PVP/PVA hydrogels for articular cartilage replacement. *Mater. Sci. Eng., C* **2009**, *29* (6), 1979−1983.

(3) Chaouat, M.; Le Visage, C.; Baille, W. E.; Escoubet, B.; Chaubet, F.; Mateescu, M. A.; Letourneur, D. A Novel Cross-Linked Poly(vinyl alcohol) (PVA) for Vascular Grafts. *Adv. Funct. Mater.* **2008**, *18*, 2855−2861.

(4) Winterton, L. C.; Lally, J. M.; Sentell, K. B.; Chapoy, L. L. The elution of poly (vinyl alcohol) from a contact lens: The realization of a time release moisturizing agent/artificial tear. *J. Biomed. Mater. Res., Part B* **2007**, *80B* (2), 424−432.

(5) Poole, T. R. G.; Gillespie, I. H.; Knee, G.; Whitworth, J. Microscopic fragmentation of ophthalmic surgical sponge spears used for delivery of antiproliferative agents in glaucoma filtering surgery. *Br. J. Ophthalmol.* **2002**, *86* (12), 1448−1449.

(6) Hassan, C.; Peppas, N. Structure and Applications of Poly(vinyl alcohol) Hydrogels Produced by Conventional Crosslinking or by Freezing/Thawing Methods. In *Biopolymers: PVA Hydrogels, Anionic Polymerisation Nanocomposites*; Advances in Polymer Science Series; Springer: Berlin, 2000; Vol. *153*, pp 37−65.

(7) Moukwa, M.; Youn, D.; Hassanali, M. Effects of degree of polymerization of water soluble polymers on concrete properties. *Cem. Concr. Res.* **1993**, *23*, 122−130.

(8) Termonia, Y.; Meakin, P.; Smith, P. Theoretical study of the influence of the molecular weight on the maximum tensile strength of polymer fibers. *Macromolecules* **1985**, *18* (11), 2246−2252.

(9) Mohsin, M.; Hossin, A.; Haik, Y. Thermal and mechanical properties of poly(vinyl alcohol) plasticized with glycerol. *J. Appl. Polym. Sci.* **2011**, *122* (5), 3102−3109.

DOI: 10.1021/acs.langmuir.5b03758
Langmuir 2016, 32, 864−872

(10) Hariharan, A.; Kumar, S. K.; Russell, T. P. Reversal of the Isotopic Effect in the Surface Behavior of Binary Polymer Blends. *J. Chem. Phys.* **1993**, *98* (5), 4163−4173.
(11) Hunter, R. J. *Foundations of Colloid Science*; Clarendon Press: Oxford, U.K., 1987.
(12) Geoghegan, M.; Jones, R. A. L.; Clough, A. S. Surface directed spinodal decomposition in a partially miscible polymer blend. *J. Chem. Phys.* **1995**, *103* (7), 2719−24.
(13) Campbell, R. A.; Edler, K. J. Growth-collapse mechanism of PEI-CTAB films at the air−water interface. *Soft Matter* **2011**, *7* (23), 11125−11132.
(14) Edler, K. J.; Wasbrough, M. J.; Holdaway, J. A.; O'Driscoll, B. M. D. Self-Assembled Films Formed at the Air−Water Interface from CTAB/SDS Mixtures with Water-Soluble Polymers. *Langmuir* **2009**, *25* (7), 4047−4055.
(15) Lu, J. R.; Li, Z. X.; Thomas, R. K.; Binks, B. P.; Crichton, D.; Fletcher, P. D. I.; McNab, J. R.; Penfold, J. The Structure of Monododecyl Pentaethylene Glycol Monolayers with and without Added Dodecane at the Air/Solution Interface: A Neutron Reflection Study. *J. Phys. Chem. B* **1998**, *102* (30), 5785−5793.
(16) Lu, J. R.; Hromadova, M.; Thomas, R. K.; Penfold, J. Neutron reflection from triethylene glycol monododecyl ether adsorbed at the air−liquid interface: The variation of the hydrocarbon chain distribution with surface concentration. *Langmuir* **1993**, *9* (9), 2417−2425.
(17) Thompson, R. L. Surface and Interface Characterization: Ion Beam Analysis. In *Polymer Science: A Comprehensive Reference*, Matyjaszewski, K., Möller, M., Eds.; Elsevier BV: Amsterdam, 2012; Vol. *2*, pp 661−681.
(18) Composto, R. J.; Walters, R. M.; Genzer, J. Application of ion scattering techniques to characterize polymer surfaces and interfaces. *Mater. Sci. Eng., R* **2002**, *38*, 107−180.
(19) Barradas, N. P.; Jeynes, C.; Webb, R. P. Simulated annealing analysis of Rutherford backscattering data. *Appl. Phys. Lett.* **1997**, *71* (2), 291−293.
(20) Möller, W.; Besenbacher, F. Note on the ^{3}He + D Nuclear-Reaction Cross Section. *Nucl. Instrum. Methods* **1980**, *168* (1−3), 111−114.
(21) Jeynes, C.; Barradas, N. P.; Szilágyi, E. Accurate Determination of Quantity of Material in Thin Films by Rutherford Backscattering Spectrometry. *Anal. Chem.* **2012**, *84* (14), 6061−6069.
(22) Jeynes, C.; Bailey, M. J.; Bright, N. J.; Christopher, M. E.; Grime, G. W.; Jones, B. N.; Palitsin, V. V.; Webb, R. P. "Total IBA"—Where are we? *Nucl. Instrum. Methods Phys. Res., Sect. B* **2012**, *271*, 107−118.
(23) Barradas, N. P.; Jeynes, C. Advanced physics and algorithms in the IBA DataFurnace. *Nucl. Instrum. Methods Phys. Res., Sect. B* **2008**, *266* (8), 1875−1879.
(24) Bucknall, D. G.; Butler, S. A.; Higgins, J. S. Studying polymer interfaces using neutron reflection. In *Scattering from Polymers*; Hsiao, B. S., Lohse, D. J., Cebe, P., Eds.; ACS Symposium Series; American Chemical Society: Washington, DC, 2000; Vol. *739*, pp 57−73.10.1021/bk-2000-0739.ch004
(25) James, C. D.; Jeynes, C.; Barradas, N. P.; Clifton, L.; Dalgliesh, R. M.; Smith, R. F.; Sankey, S. W.; Hutchings, L. R.; Thompson, R. L. Modifying Polyester Surfaces with Incompatible Polymer Additives. *React. Funct. Polym.* **2015**, *89*, 40−48.
(26) Hardman, S. J.; Hutchings, L. R.; Clarke, N.; Kimani, S. M.; Mears, L. L. E.; Smith, E. F.; Webster, J. R. P.; Thompson, R. L. Surface Modification of Polyethylene with Multi-End-Functional Polyethylene Additives. *Langmuir* **2012**, *28* (11), 5125−5137.
(27) Payne, R. S.; Clough, A. S.; Murphy, P.; Mills, P. J. Use of the D(^{3}He,P)^{4}He Reaction to Study Polymer Diffusion in Polymer Melts. *Nucl. Instrum. Methods Phys. Res., Sect. B* **1989**, *42* (1), 130−134.
(28) Barradas, N. P. Rutherford backscattering analysis of thin films and superlattices with roughness. *J. Phys. D: Appl. Phys.* **2001**, *34* (14), 2109−2116.
(29) Su, J.-F.; Huang, Z.; Liu, K.; Fu, L.-L.; Liu, H.-R. Mechanical Properties, Biodegradation and Water Vapor Permeability of Blend Films of Soy Protein Isolate and Poly (vinyl alcohol) Compatibilized by Glycerol. *Polym. Bull.* **2007**, *58* (5−6), 913−921.
(30) Sakellariou, P.; Hassan, A.; Rowe, R. C. Plasticization of aqueous poly(vinyl alcohol) and hydroxypropyl methylcellulose with polyethylene glycols and glycerol. *Eur. Polym. J.* **1993**, *29* (7), 937−943.
(31) Hariharan, A.; Kumar, S. K.; Russell, T. P. A lattice model for the surface segregation of polymer chains due to molecular weight effects. *Macromolecules* **1990**, *23* (15), 3584−3592.
(32) Brandrup, J., Immergut, E. H., Eds. *Polymer Handbook*, 3rd ed.; Wiley-Interscience: Chichester, U.K., 1989.
(33) Marten, F. L. Vinyl Alcohol Polymers. In *Kirk-Othmer Encyclopedia of Chemical Technology* [Online]; John Wiley & Sons, Posted Jun 10, 2002. http://onlinelibrary.wiley.com/doi/10.1002/0471238961.2209142513011820.a01.pub2/abstract; accessed January 2016.
(34) Polmanteer, K. E. Current perspectives on silicone rubber technology. *Rubber Chem. Technol.* **1981**, *54* (5), 1051−1080.
(35) Wu, S. Estimation of the critical surface tension for polymers from molecular constitution by a modified Hildebrand−Scott equation. *J. Phys. Chem.* **1968**, *72*, 3332.
(36) Lee, L. H. Relationships between surface wettability and glass temperatures of high polymers. *J. Appl. Polym. Sci.* **1968**, *12*, 719.
(37) van Krevelen, D. W.; Hoftyzer, P. J. *Properties of Polymers, their estimation and correlation with chemical structure*, 2nd ed.; Elsevier, Amsterdam, 1976.
(38) van Oss, C. J.; Chaudhury, M. K.; Good, R. J. Monopolar surfaces. *Adv. Colloid Interface Sci.* **1987**, *28*, 35−64.
(39) Takamura, K.; Fischer, H.; Morrow, N. R. Physical properties of aqueous glycerol solutions. *J. Pet. Sci. Eng.* **2012**, *98*−*99*, 50−60.
(40) Adamczyk, Z.; Para, G.; Warszyński, P. Influence of Ionic Strength on Surface Tension of Cetyltrimethylammonium Bromide. *Langmuir* **1999**, *15* (24), 8383−8387.
(41) Cuny, V.; Antoni, M.; Arbelot, M.; Liggieri, L. Structural properties and dynamics of C12E5 molecules adsorbed at water/air interfaces: A molecular dynamic study. *Colloids Surf., A* **2008**, *323* (1−3), 180−191.
(42) Kjellin, U. R. M.; Claesson, P. M.; Linse, P. Surface Properties of Tetra(ethylene oxide) Dodecyl Amide Compared with Poly(ethylene oxide) Surfactants. 1. Effect of the Headgroup on Adsorption. *Langmuir* **2002**, *18* (18), 6745−6753.
(43) Jones, R. A. L.; Norton, L. J.; Kramer, E. J.; Bates, F. S.; Wiltzius, P. Surface-directed spinodal decomposition. *Phys. Rev. Lett.* **1991**, *66* (10), 1326−1329.
(44) Bruder, F.; Brenn, R. Spinodal Decomposition in Thin Films of a Polymer Blend. *Phys. Rev. Lett.* **1992**, *69* (4), 624−627.
(45) Krausch, G.; Dai, C. A.; Kramer, E. J.; Marko, J. F.; Bates, F. S. Interference of Spinodal Waves in Thin Polymer Films. *Macromolecules* **1993**, *26* (21), 5566−5571.

DOI: 10.1021/acs.langmuir.5b03758
Langmuir 2016, 32, 864−872